

Premature aggregation of type IV collagen and early lethality in lysyl hydroxylase 3 null mice

Kati Rautavuoma^{*††}, Kati Takaluoma^{*††}, Raija Sormunen[§], Johanna Myllyharju^{*†}, Kari I. Kivirikko^{*†}, and Raija Soininen^{†¶}

^{*}Collagen Research Unit and Departments of [†]Medical Biochemistry and Molecular Biology and [§]Pathology, Biocenter Oulu, University of Oulu, 90014 Oulu, Finland

Edited by Erkki Ruoslahti, The Burnham Institute, La Jolla, CA, and approved August 17, 2004 (received for review July 9, 2004)

Collagens carry hydroxylysine residues that act as attachment sites for carbohydrate units and are important for the stability of crosslinks but have been regarded as nonessential for vertebrate survival. We generated mice with targeted inactivation of the gene for one of the three lysyl hydroxylase isoenzymes, LH3. The null embryos developed seemingly normally until embryonic day 8.5, but development was then retarded, with death around embryonic day 9.5. Electron microscopy (EM) revealed fragmentation of basement membranes (BMs), and immuno-EM detected type IV collagen within the dilated endoplasmic reticulum and in extracellular aggregates, but the typical BM staining was absent. Amorphous intracellular and extracellular particles were also seen by collagen IV immunofluorescence. SDS/PAGE analysis demonstrated increased mobilities of the type IV collagen chains, consistent with the absence of hydroxylysine residues and carbohydrates linked to them. These results demonstrate that LH3 is indispensable for biosynthesis of type IV collagen and for BM stability during early development and that loss of LH3's functions leads to embryonic lethality. We propose that the premature aggregation of collagen IV is due to the absence of the hydroxylysine-linked carbohydrates, which thus play an essential role in its supramolecular assembly.

Lysyl hydroxylase (LH, EC 1.14.11.4, *Plod*) catalyzes the hydroxylation of lysine residues in -X-Lys-Gly- triplets in collagens and other proteins with collagen-like sequences (1). The hydroxylysine residues formed have two important functions: (i) they serve as attachment sites for carbohydrates, either monosaccharide galactose or disaccharide glucosylgalactose, and (ii) they have an important role in the stabilization of intermolecular collagen crosslinks that provide tensile strength and mechanical stability for the collagen fibrils. The extent of lysine hydroxylation and hydroxylysine glycosylation varies between collagen types. Nearly 90% of all lysines are hydroxylated and hydroxylysines glycosylated in types IV and VI collagen, whereas <20% of the lysines are hydroxylated in type III collagen (2). The functions of the hydroxylysine-linked carbohydrates are poorly understood, but in the case of fibril-forming collagens, they are thought to regulate the formation and morphology of the fibrils (1, 3).

Three human LH isoenzymes have been identified (1, 4–6). Mutations in the LH1 gene lead to the kyphoscoliotic type of Ehlers–Danlos syndrome, which is characterized by scoliosis, joint laxity, skin fragility, ocular manifestations, and severe muscle hypotonia (7–9). Mutations in the LH2 gene have recently been reported in two families with Bruck syndrome, which is characterized by fragile bones, joint contractures, scoliosis, and osteoporosis (10).

No mutations have been characterized in the gene for the isoenzyme LH3, and its *in vivo* functions have not yet been elucidated. This protein differs from the other two lysyl hydroxylase isoenzymes in that it also possesses relatively low levels of collagen glucosyltransferase activity and very small amounts of collagen galactosyltransferase activity in addition to the lysyl hydroxylase activity (11–13). In this study, we generated mice with targeted inactivation of the LH3 (*Plod3*) gene and show that

LH3 is essential for the synthesis of type IV collagen during early development and, hence, for the stability of basement membranes (BMs).

Materials and Methods

Targeting of the *Plod3* Gene and Generation of Mutant Mice. The genomic clone used to clone the targeting construct was isolated from a 129SV mouse genomic library with human LH3 cDNA (5) as a probe. The construct contains 1.2- and 5-kb genomic arms and the β -gal-PGK-*neo* cassette inserted in-frame into exon 1. Embryonic stem cells were targeted, and mice were generated by standard techniques. The embryonic stem cells and mice were genotyped by PCR with primers from the *PGK* promoter, the *Plod3* promoter, and exon 6 of the *Plod3* gene. For Southern blotting, genomic DNA was digested with *Hind*III and hybridized with the 3' genomic fragment. Animal experiments were approved by the Animal Research Committee of the University of Oulu, Oulu, Finland.

RNA Isolation and RT-PCR. Total RNA was extracted from embryonic day (E) 9.5 embryos by using Tri Reagent (Sigma), and Northern blots were prepared by routine methods. The membrane was hybridized with an LH3 cDNA probe containing exons 2–19, and the integrity of the RNA was confirmed by hybridization with a β -actin probe. For RT-PCR, the first strand was synthesized with oligo(dT) as a universal primer, and primers from (i) the 5' untranslated region and exon 2 of the *Plod3* gene, (ii) the 5' end of the *PGK* promoter and exon 2 of the *Plod3* gene, and (iii) exons 2 and 19 of the *Plod3* gene were used for the subsequent amplifications. RT-PCR products were sequenced with the DYEnamic ET Terminator Cycle Sequencing kit (Amersham Biosciences) and analyzed in an automatic sequencer.

Histology and Immunofluorescence. Embryos were collected from heterozygous females 8 or 9 days after detection of the copulation plug, the placentas or yolk sacs were dissected for DNA isolation, and the embryos were either snap-frozen in isopentane cooled in liquid nitrogen or fixed in neutral formalin and processed for paraffin sectioning. 5-Bromo-4-chloro-3-indolyl β -D-galactoside (X-Gal) staining of embryos and tissues of adult mice was performed as described in ref. 14, followed by fixation and processing for paraffin sectioning. Immunofluorescence studies were carried out on frozen sections by using the monoclonal rat anti-laminin B2 chain (γ 1) (Chemicon), polyclonal rabbit anti-mouse collagen IV (Chemicon), and monoclonal rat anti-HS proteoglycan (Seikagaku, Tokyo). Labeled secondary

This paper was submitted directly (Track II) to the PNAS office.

Abbreviations: BM, basement membrane; EM, electron microscopy; En, embryonic day *n*; ER, endoplasmic reticulum; LH, lysyl hydroxylase; X-Gal, 5-bromo-4-chloro-3-indolyl β -D-galactoside.

[†]K.R. and K.T. contributed equally to this work.

[¶]To whom correspondence should be addressed. E-mail: raija.soininen@oulu.fi.

© 2004 by The National Academy of Sciences of the USA

antibodies were Cy2 (Jackson ImmunoResearch) or Alexa Fluor (Molecular Probes).

Transmission and Immuno-Electron Microscopy (EM). Whole E9.5 embryos were fixed in 2.5% glutaraldehyde in 0.1 M phosphate buffer and postfixed in 1% osmium tetroxide. For immun-EM, embryos were fixed in 4% paraformaldehyde in a 0.1 M phosphate buffer with 2.5% sucrose. They were then cut horizontally, and both the anterior and posterior regions were analyzed. Pieces were immersed in 2.3 M sucrose and were frozen in liquid nitrogen. For immunolabeling, thin cryosections were incubated with the collagen IV antibody (Chemicon) and then with protein A-gold complex. Sections were examined in a Philips CM100 transmission electron microscope (FEI, Eindhoven, The Netherlands).

Western Analysis. E9.5 embryos were homogenized in homogenization buffer (0.2 M NaCl/0.1 M glycine/0.1% Triton X-100/50 μ M DTT/20 mM Tris, pH 7.5). The proteins were separated on a 6% SDS/PAGE gel and transferred to a poly(vinylidene difluoride) membrane. The membrane was blocked with 5% milk and incubated with the collagen IV antibody (Rockland, Gilbertsville, PA) and then with horseradish peroxidase-linked goat anti-rabbit secondary antibody (Caltag, South San Francisco, CA). Immunocomplexes were visualized by using ECL reagents (Amersham Biosciences).

Enzyme Activity Measurements. E9.5 embryos were homogenized in homogenization buffer, the protein concentration was determined, and the enzyme activities were measured as described in ref. 15. LH activity was determined with a [14 C]lysine-labeled type I procollagen substrate. Collagen galactosyltransferase and glucosyltransferase were assayed based on the transfer of

Table 1. Genotypes of embryos obtained from *Plod3* heterozygote intercrosses

| Embryonic stage | <i>n</i> | +/+ | +/- | -/- |
|-----------------|----------|----------|-----------|----------|
| E8.5 | 163 | 41 (25%) | 81 (50%) | 41 (25%) |
| E9.5 | 253 | 71 (28%) | 135 (53%) | 47 (19%) |
| E10.5 | 87 | 32 (37%) | 49 (56%) | 6 (7%) |

[14 C]galactose or [14 C]glucose from radioactive UDP-galactose or UDP-glucose to hydroxylysine or galactosylhydroxylysine residues, respectively, in a denatured citrate-soluble rat-skin collagen substrate.

Results

Generation of LH3 Null Embryos, Their Histology, and X-Gal Staining.

The murine *Plod3* gene was disrupted by inserting the *lacZ- β PGK-neo* cassette into exon 1 so that the bacterial β -galactosidase reporter was under the control of the *Plod3* promoter (Fig. 1). More than 20 embryonic stem cell clones with the targeted mutation were identified, three of which were injected into mouse blastocysts, resulting in high-level chimerism and germline transmission. All three lines showed the same phenotype. Heterozygous mice that had no symptoms were interbred to produce homozygous mutants. Because genotyping of the offspring revealed that only wild-type and heterozygous mice are viable, embryos at different developmental stages were analyzed (Table 1). The LH3 null embryos were found to develop seemingly normally until E8.5, after which their development was retarded. At E9.5, they were very fragile and \approx 60% of the size of the wild-type and heterozygous embryos (Fig. 2A). A null embryo with a beating heart could occasionally be recovered at

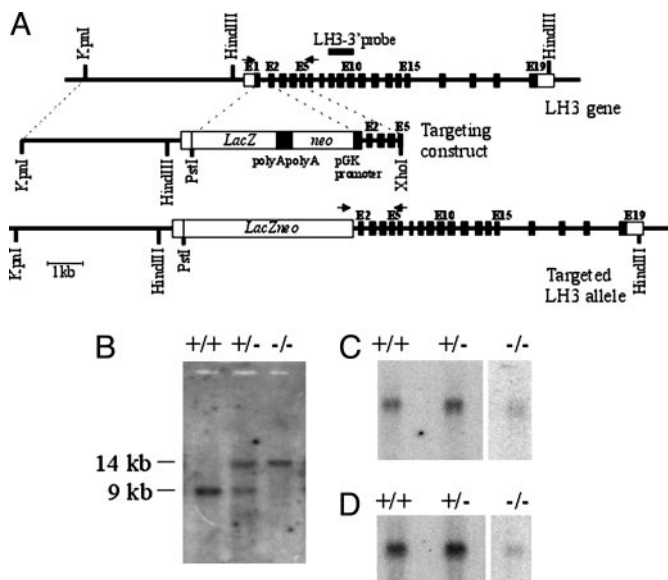


Fig. 1. Disruption of the LH3 (*Plod3*) gene in mice. (A) The *Plod3* gene contains 19 exons (Top), and the *lacZ-neo* cassette was inserted into exon 1 so that the *neo* gene was in the opposite orientation and was driven by the *PGK* promoter. The locations of the primers used in genotyping are indicated by arrows, and the location of the probe used in the Southern hybridization is indicated by a bar. (B) Southern analysis of *Hind*III-digested DNA from E9.5 embryos. (C and D) Northern analysis of total embryonic RNA hybridized with the LH3 (C) and β -actin (D) probes. RNA obtained from one wild-type or heterozygous embryo and from four LH3 null embryos was loaded into the gel. The signal detected in the *Plod3*^{-/-} lane (C) was analyzed by RT-PCR and turned out to represent a nonfunctional transcript (see Results).

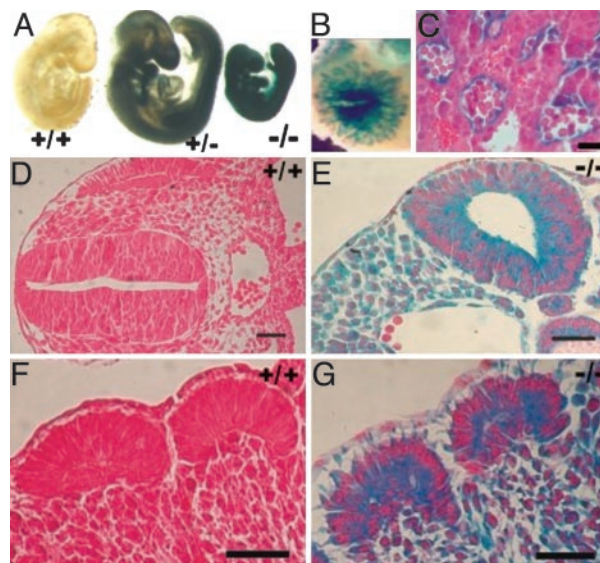


Fig. 2. X-Gal staining of E9.5 embryos. (A) *Plod3* heterozygote and null embryos are intensely stained. The null embryos are smaller in size, but no obvious developmental abnormalities are visible. (B) The labyrinth layer of the placenta of an E9.5 LH3 null embryo is intensely stained (stereomicroscopic view). (C) The staining (blue) is localized in the walls of the embryonic blood vessels in a section through the placenta shown in B. (D and E) Anterior region of wild-type (D) and null (E) embryo, oblique sections. Intense staining is observed in the mesenchyme, neuroepithelium, and endothelial cells of the null embryo. (F and G) The somite region with lower cell density and separation of cells in the mesenchyme surrounding the somites in the null embryo (G). Sections were counterstained with hematoxylin/eosin (C) or eosin (D–G). (Scale bars: C, 50 μ m; D–G, 200 μ m.)

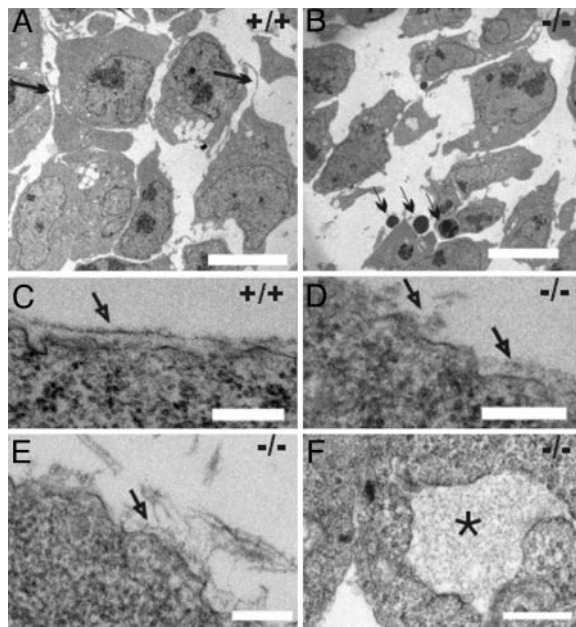


Fig. 3. Transmission EM of E9.5 embryos. (A) The mesodermal cells of the wild-type embryo are densely packed and have long filopodia (arrows). (B) The mesodermal cells of LH3 null embryos are sparse, contacts are rare, and the cells have fewer filopodia. Apoptotic nuclei (thin arrows) are frequently found. (C) Well formed BMs in the ectoderm of a wild-type embryo (arrow). (D and E) The BM in the null mutant is fragmented and detached from the cell surface (arrows). (F) Dilated ER (*) in a null mutant cell. (Scale bars: A and B, 10 μm ; C–E, 200 nm; F, 500 nm.)

E10.5 (Table 1), but these were so fragile that they could not be touched without disruption.

The amounts of intact RNA obtained from the mutant embryos were small; still, a band was seen in Northern hybridization when the 3' end of the LH3 cDNA was used as a probe (Fig. 1C). Sequence analysis of an oligo(dT)-primed, PCR-amplified product showed that the transcript starts from the antisense strand of the PGK promoter or 5' region of the *neo* gene (the exact transcription start site was not analyzed), carries part of the *Plod3* intron 2, and contains the *Plod3* exon sequences downstream. A continuous reading frame is found only in the LH3 coding region, where the first codon for methionine, corresponding to residue 99 in the processed LH3 polypeptide, is 560 bp from the start of the amplified product, and the sequence closest to the Kozak consensus is located 1,399 bp from the start of the sequence, corresponding to methionine 379 in the processed polypeptide. The product of RT-PCR with RNA isolated from wild-type embryos contained a complete LH3 cDNA sequence.

Hypothetically, a truncated polypeptide could be translated from the aberrant transcript, but this is unlikely, because its 5' end carries a long stretch of antisense PGK and intron sequences. Furthermore, even if a polypeptide were synthesized, it would be unlikely to be correctly folded and would contain no signal sequence. An analogous situation has been reported for the *Men1* gene, where the aberrant transcript had a dominant-negative effect (16). In the case of LH3, no negative effects were observed in heterozygotes, supporting our assumption that this transcript is nonfunctional. The main difference between the two cases is that in the *Men1* targeting, the *PGK-neo* cassette was inserted so that all of the intron sequences were spliced out, whereas in LH3 targeting this was not the case.

Northern analysis and RT-PCR showed that mRNAs for LH1 and LH2 were also expressed in wild-type, heterozygote, and null

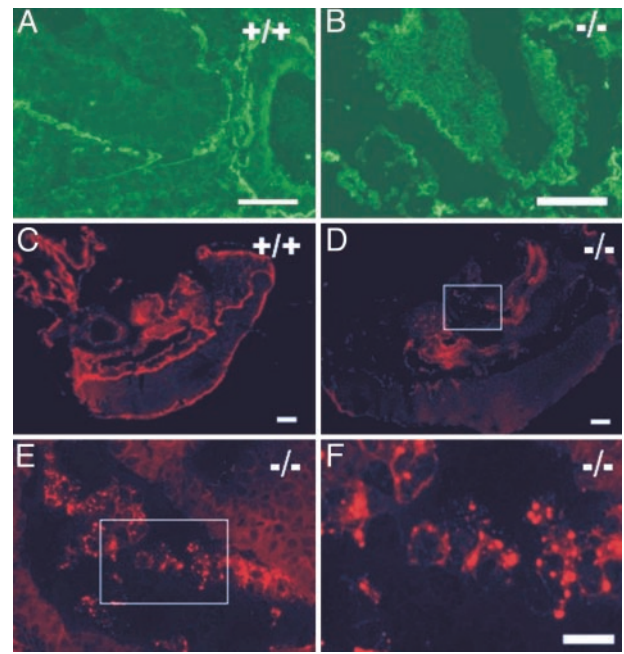


Fig. 4. Visualization of BMs by immunofluorescence. (A) The laminin $\gamma 1$ antibody shows continuous BM staining in the wild-type E9.5 embryo. (B) The BMs in the E9.5 LH3 null mutant appear to be thinner in laminin $\gamma 1$ staining and are fragmented in some areas. (C) Intense BM staining of a wild-type E8.5 embryo with the collagen IV antibody. (D–F) Weak, spotty staining with the collagen IV antibody in an E8.5 LH3 null embryo. (E and F) Higher magnification of the boxed area in D reveals brightly stained particles in the null embryo section. (Scale bars: A and B, 50 μm ; C and D, 100 μm ; F, 10 μm .)

embryos, with no apparent differences in the mRNA levels between the three types (data not shown).

Histological examination of the E9.5 LH3 null embryos showed a considerably lower cell density than in controls (Fig. 2 D–G), but no specific developmental abnormalities were observed. X-Gal staining was performed to study *Plod3* promoter-driven β -galactosidase expression, showing intense and ubiquitous staining in the heterozygous and null embryos (Fig. 2 A, E, and G) at E8.5–E9.5. The walls of all of the blood vessels in both the placenta and the embryo proper were also intensely stained (Fig. 2 C and E).

Fragmentation of BMs in LH3 Null Embryos. Transmission EM of the E9.5 embryos revealed that the wild-type embryos had continuous BMs with a lamina lucida and lamina densa, whereas the null mutants lacked any continuous BMs. Instead, BM fragmentation, stretches of amorphous deposits on the cell surfaces, and detachment of BMs in some areas were seen (Fig. 3 C–E). Inspection of the cell organelles of the LH3 null embryos revealed dilation of the endoplasmic reticulum (ER) (Fig. 3F), enlarged Golgi complexes with dilated stacks, and enlarged lysosomes (not shown).

Immunofluorescence showed continuous intense BM staining patterns with antibodies against laminin (Fig. 4A), perlecan (not shown), and type IV collagen (Fig. 4C) in the wild-type embryos at E8.5–E9.5. The BMs of mutant embryos stained for the laminin $\gamma 1$ chain and perlecan at E9.5, although they seemed somewhat thinner and more fragmented (Fig. 4B). Staining for type IV collagen was weak or almost absent in the null mutants, but brightly stained, unusual intracellular and extracellular amorphous particles were observed (Fig. 4 D–F). These particles were not detected with the other BM markers.

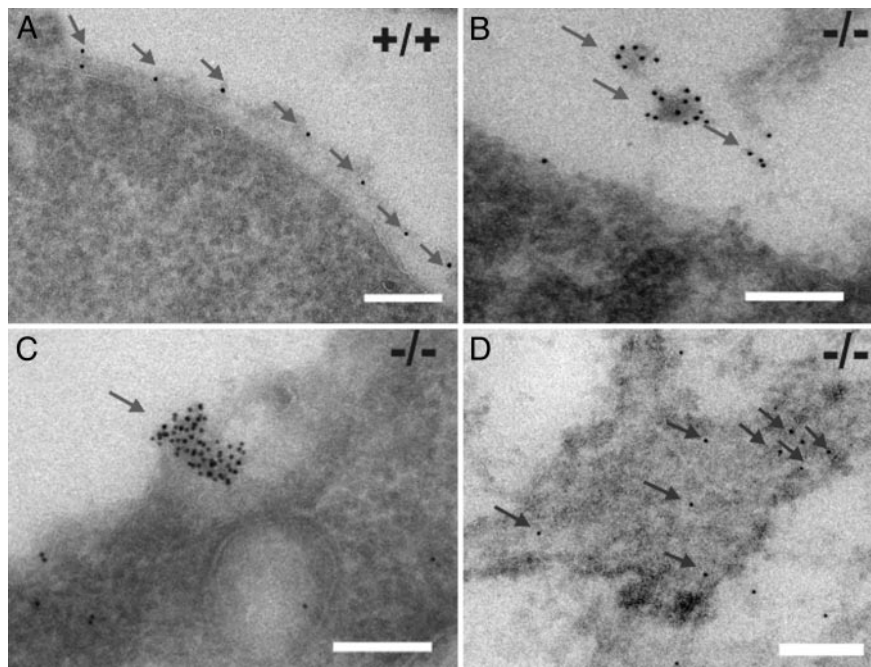


Fig. 5. Type IV collagen immuno-EM of E9.5 embryos. (A) Gold particles decorate the BM zone in the wild-type sample. (B) LH3 null embryos lack the typical BMs. Heavily labeled amorphous deposits are detected in the extracellular space. (C) An intensely labeled aggregation in a secretion vesicle at the cell surface in an LH3 null embryo. (D) Numerous single gold particles in the dilated ER of an LH3 null embryo. (Scale bars: 200 nm.)

Type IV Collagen Synthesis Is Affected in LH3 Null Embryos. Type IV collagen localization was further characterized by immuno-EM, through which antibodies against type IV collagen showed decoration of the BM zone in the wild-type and heterozygous embryos (Fig. 5A). In the null embryos, gold particles were seen in the aggregated material in the extracellular space (Fig. 5B) and in the secretion vesicles being deposited from the cells (Fig. 5C) but not in the BM zone. Gold particles were also detected in the dilated ER (Fig. 5D).

Western analysis demonstrated that the quantity of type IV collagen synthesized in the LH3 null embryos is unchanged, but migration of the $\alpha 1(\text{IV})$ and $\alpha 2(\text{IV})$ chains in null mutants was faster than in the wild-type embryos; the mobility of $\alpha 1(\text{IV})$ in the mutant corresponded to that of the 170-kDa $\alpha 2(\text{IV})$ in the wild type, instead of 185 kDa (Fig. 6). The apparent reductions in the molecular weights of the $\alpha 1(\text{IV})$ and $\alpha 2(\text{IV})$ chains are in good agreement with the calculated losses of about 16 and 13 kDa, respectively, assuming a complete absence of hydroxylysine and its carbohydrate units in the two types of chain.

Enzyme-activity assays were performed by using E9.5 embryo lysates, although comparison of the activities cannot be accurate because of the developmental retardation of the null embryos and the size difference (Fig. 2A). No difference was found in the level of total lysyl hydroxylase activity per unit of total protein when measured with a substrate consisting of nonhydroxylated polypeptide chains of type I procollagen (ref. 15 and data not shown), but it is currently unknown whether this substrate measures preferentially the activities of LH1 and LH2. No difference was seen in the level of collagen galactosyltransferase activity either, whereas the level of collagen glucosyltransferase activity was decreased by $\approx 85\%$ in the null embryos.

Expression of LH3 in Tissues During Normal Development as Detected by X-Gal Staining. Because X-Gal staining of the E8.5–E9.5 heterozygote embryos was almost as intense as in the null homozygotes (Fig. 2A), it was regarded as feasible for the analysis of LH3 expression during normal development. The

widespread LH3 expression seen during early embryogenesis (Fig. 7A) was found to become more restricted at later stages. In the eye, for instance, a very intense staining is seen in the developing lens at E12.5, but the intensity decreases during development (Fig. 7B–D), and the expression is found in the lens epithelial cells and faintly in the ciliary body at the adult stage (Fig. 7E). Expression is also seen in the vitreal surface of the retina in embryos, whereas staining in the adult eye is mainly localized in the capillaries of the retina and the inner segment of the photoreceptors (Fig. 7D and F). Staining is strong in the developing bones at E12.5 (Fig. 7B), being localized in the chondrocytes (Fig. 7G), where it is seen throughout life (Fig. 7H). Perimysia, the capillaries, and arterial walls are stained in adult tissues (Fig. 7I–L). In the kidney, intense staining is seen

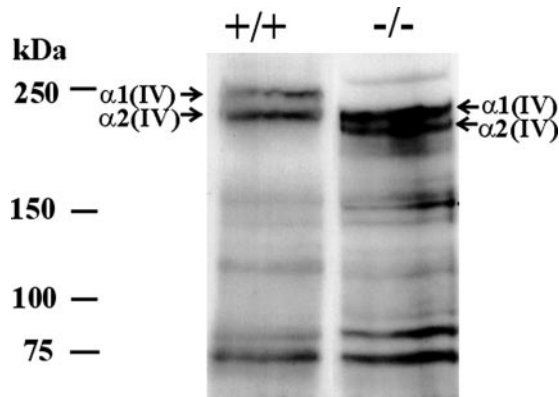


Fig. 6. Western analysis of type IV collagen in E9.5 wild-type and LH3 null embryo lysates, demonstrating enhanced migration of collagen $\alpha 1(\text{IV})$ and $\alpha 2(\text{IV})$ chains in the latter. The apparent reductions in the molecular masses of the two types of chain in the null lysates correspond to a total loss of hydroxylysine and its carbohydrate units. The polypeptides with apparent molecular masses of ≈ 75 kDa probably represent degradation products of the full-length chains. The amount of total protein loaded into the gel was 70 μg .

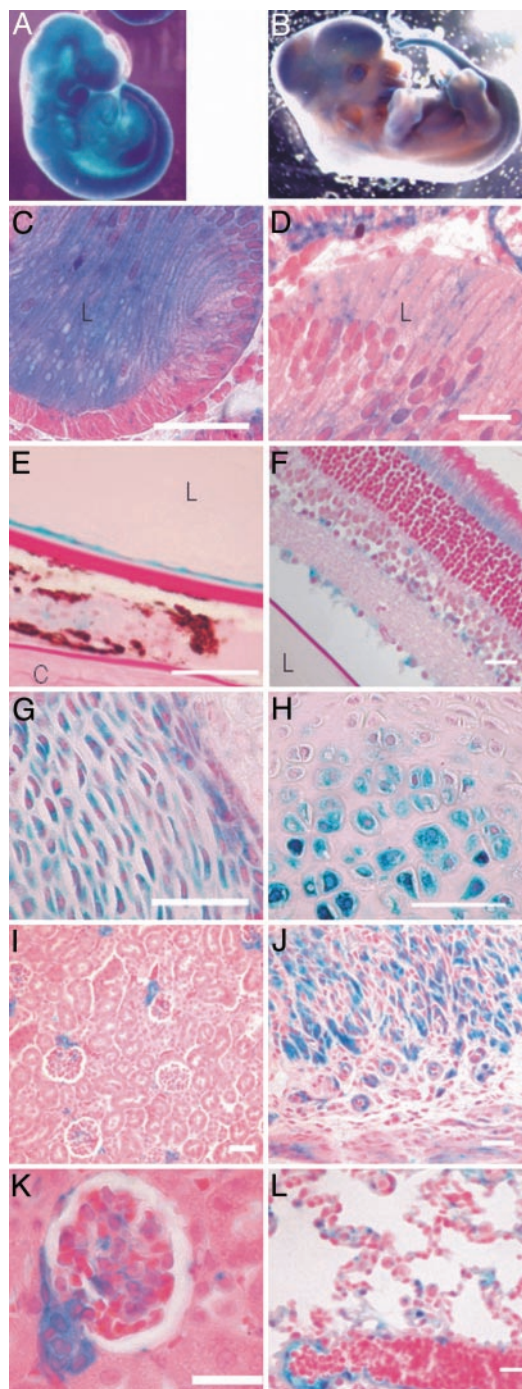


Fig. 7. X-Gal staining of *Plod3* heterozygote embryos and tissues. (A) Ubiquitous staining in an E9.5 embryo; a stereomicroscopic view. (B) An E12.5 embryo; a stereomicroscopic view. Staining is intense in the head region, the lens, and the developing bones. (C) Histological section of the intensely stained E12.5 lens. (D) Staining of the lens is considerably weaker at E14.5. Staining is also seen in the vitreal surface of the retina. (E) Anterior region of the adult eye. The lens epithelial cells are intensely stained, and weaker staining is detected in the ciliary body (flanked by the cornea and the lens). (F) Staining of the capillaries and the photoreceptor layer of the retina is seen in the posterior region of the adult eye. (G) Chondrocytes in the developing bone of an E14.5 embryo show specific staining. (H) Staining is intense also in the chondrocytes of a 5-week-old mouse. (I and K) Staining in the kidney of a 1-month-old mouse is detected mainly in the mesangium and the vascular pole of the glomerulus. (J) Capillary walls and the perimysia are stained in the uterus of a 1.5-year-old mouse. (L) In the lungs, staining is localized in the alveolar capillaries and blood vessel walls. Sections were stained with hematoxylin/eosin or with periodic acid/Schiff reagent (E and F). L, lens; C, cornea. (Scale bars: C–H, K, and L, 50 μm ; I and J, 100 μm .)

in the vascular poles and mesangia of the glomeruli, and weaker, punctuate staining is seen in tubuli (Fig. 7 I and K). Intense staining is also found around the nerves and in the adrenal gland; single hepatocytes are occasionally stained in the liver (not shown).

Discussion

No data have been available on the significance of lysine hydroxylation in collagen types that do not form fibrils (17). Our present results show that absence of LH isoenzyme LH3 leads to early embryonic lethality because of its essential role in the synthesis of type IV collagen. The function of LH3 is probably connected with the glycosylation of collagen chains, although an abnormal crosslinking of the hydroxylysine-deficient type IV collagen may contribute to the fragmentation of BMs. Our results thus suggest a major role for the hydroxylysine-linked carbohydrate units in the supramolecular assembly of collagen IV.

Type IV collagen molecules spontaneously assemble in a complex polygonal network by lateral associations and interactions at the C- and N-terminal domains, with the C-terminal globular domains forming dimers and the N-terminal domains forming tetramers by parallel and antiparallel alignment (18, 19). Asparagine-linked oligosaccharides, and possibly also hydroxylysine-linked disaccharides, have been suggested as determinants of the alignment of the monomers at the N terminus (20), but no data are available to indicate how the lateral interactions between triple-helical regions are formed and regulated.

Our results show that a portion of the type IV collagen synthesized in the LH3 null embryos is retained and probably degraded in the ER or trafficked for degradation in lysosomes, which are enlarged in the null mutants. Western analyses indicated alterations in the mobility of the $\alpha 1(\text{IV})$ and $\alpha 2(\text{IV})$ chains, with the differences between the wild-type and null samples being consistent with a total absence of hydroxylysine and its carbohydrates. Immunofluorescence showed the presence of amorphous intracellular and extracellular type IV collagen particles. Immuno-EM verified the aggregation of the newly synthesized type IV collagen and indicated that aggregation of the deficiently modified type IV collagen occurs on the way to the cell surface, because tight, intensely stained aggregates were seen in the secretion vesicles but not in the ER. These findings cannot be due to abnormalities in the crosslinking of the hydroxylysine-deficient type IV collagen, because the crosslinks are only formed gradually in the extracellular matrix (17). However, the possibility is not excluded that an abnormal crosslinking contributed to the formation of the extracellular type IV collagen aggregates and hence to the fragmentation of the BMs. Our results imply that LH3 is the main LH isoenzyme involved in the synthesis of type IV collagen during early vertebrate development, because the two other LH isoenzymes, LH1 and LH2, which also are expressed in E7.5–E9.5 embryos, were not able to compensate for the lack of LH3.

The null embryos appear to develop normally up to E8.5 but show a general developmental retardation thereafter. In our analysis the placentas appeared normal, but the possibility cannot be excluded that inefficient function of placental vasculature where intense LH3 expression was detected may have contributed to the retardation.

Although the functions of hydroxylysine residues in the synthesis of nonfibrillar collagens in vertebrates have not been analyzed, the absence of the only LH in *Caenorhabditis elegans* has been shown to impair the secretion of type IV collagen of this nematode from cells, thus leading to its absence from BMs with a developmental arrest at the twofold stage (21). BMs are a composite of several glycoproteins and proteoglycans in which two networks, formed by laminin and type IV collagen, are thought to be the basic intermingling structures (22). Laminin, like type IV collagen, is capable of self-assembly, and absence of

the laminin $\beta 1$ (23) or $\gamma 1$ (24) chain leads to death within 1 day of implantation, at E5.5. On the other hand, absence of another ubiquitous BM component, perlecan, is lethal at E10 at the earliest (25). The BMs in our LH3 null embryos showed normal staining for laminin and perlecan and were functional enough to support early development but became fragmented at E9.5, and even though type IV collagen was synthesized, it was not incorporated into them. Interestingly, mouse embryos with a total depletion of type IV collagen develop further than LH3 null embryos: They die of BM structural deficiency between E10.5 and E11.5 (26).

It is currently unknown whether collagens other than type IV are important substrates for LH3 *in vivo*. Type XVIII collagen is associated with the BMs and expressed during early development (27). Aberrant deposition of this collagen may enhance the instability of BMs and therefore contribute to the BM fragmentation. The highly hydroxylated and glycosylated type VI collagen is enriched around BMs but is detected only after E11.5 (28); therefore, its alterations cannot be involved in the mortality of LH3 null mice. It may still be a notable substrate at later stages, where LH3 expression is not coupled exclusively with synthesis of type IV collagen.

In addition to LH activity, LH3, but not LH1 or LH2, also possesses collagen glucosyltransferase activity and very small amounts of collagen galactosyltransferase activity (11–13), implying that this protein may be able to perform all of the reactions involved in the formation of hydroxylysine and its carbohydrate units. The level of collagen galactosyltransferase activity was not decreased in the LH3 null embryos, but collagen

glucosyltransferase activity had decreased to $\approx 15\%$ in the null embryos, indicating that this activity of LH3 is of real biological significance and may contribute to the phenotype in null mice. Because some of the activity was still detected in the null embryos, other enzymes with the same catalytic activity must exist and may make a more important contribution to this function later in life.

Hydroxylysines are not essential for collagen fibril formation; recombinant type I and III collagens with no hydroxylysine form native-type fibrils *in vitro* (29, 30). Many patients with the kyphoscoliotic type of Ehlers–Danlos syndrome with mutations in the LH1 gene have a virtual absence of hydroxylysine in the collagens of their skin and some other tissues and yet have a relatively mild disease phenotype (7–9). The clinical manifestations in the kyphoscoliotic type of Ehlers–Danlos syndrome and in Bruck syndrome, where mutations in the LH2 gene were recently identified (10), are believed to be due to impaired stability of crosslinks in fibrillar collagens. Our analyses show that functions of the third isoform, LH3, are crucial with regard to both embryonic development and type IV collagen assembly. These functions appear to be mainly related to the subsequent reactions leading to the glycosylation of the hydroxylysine residues formed on the collagen chains, but changes in crosslinking may have contributed to some of the abnormalities found.

We thank Anu Myllymäki and Outi Mänty for expert technical assistance. This work was supported by Health Science Council Grants 200471 and 203574 and the Finnish Center of Excellence Program 2000–2005, Grant 44843, of the Academy of Finland.

- Kivirikko, K. I. & Pihlajaniemi, T. (1998) *Adv. Enzymol. Relat. Areas Mol. Biol.* **72**, 325–398.
- Kivirikko, K. I., Myllylä, R. & Pihlajaniemi, T. (1992) in *Posttranslational Modifications of Proteins*, eds. Harding, J. J. & Crabbe, M. (CRC, Boca Raton, FL), pp. 1–51.
- Notbohm, H., Nokelainen, M., Myllyharju, J., Fietzek, P. P., Müller, P. K. & Kivirikko, K. I. (1999) *J. Biol. Chem.* **274**, 8988–8992.
- Valtavaara, M., Papponen, H., Pirttilä, A. M., Hiltunen, K., Helander, H. & Myllylä, R. (1997) *J. Biol. Chem.* **272**, 6831–6834.
- Passoja, K., Rautavuoma, K., Ala-Kokko, L., Kosonen, T. & Kivirikko, K. I. (1998) *Proc. Natl. Acad. Sci. USA* **95**, 10482–10486.
- Valtavaara, M., Szpirer, C., Szpirer, J. & Myllylä, R. (1998) *J. Biol. Chem.* **273**, 12881–12886.
- Pinnell, S. R., Krane, S. M., Kenzora, J. E. & Glimcher, M. J. (1972) *N. Engl. J. Med.* **286**, 1013–1020.
- Yeowell, H. & Walker, L. C. (2000) *Mol. Genet. Metab.* **71**, 212–224.
- Steinmann, B., Royce, P. M. & Superti-Fuga, A. (2002) in *Connective Tissue and its Heritable Disorders: Molecular, Genetic, and Medical Aspects*, eds. Royce, P. M. & Steinmann, B. (Wiley-Liss, New York), 2nd Ed., pp. 431–523.
- van der Slot, A. J., Zuurmond, A.-M., Bardoel, A. F. J., Wijmenga, C., Pruijs, H. E. H., Sillence, D. O., Brinckmann, J., Abraham, D. J., Black, C. M., Verzijl, N., et al. (2003) *J. Biol. Chem.* **276**, 40967–40972.
- Heikkinen, J., Risteli, M., Wang, C., Latvala, J., Rossi, M., Valtavaara, M. & Myllylä, R. (2000) *J. Biol. Chem.* **275**, 36158–36163.
- Rautavuoma, K., Takaluoma, K., Passoja, K., Pirskanen, A., Kvist, A.-P., Kivirikko, K. I. & Myllyharju, J. (2002) *J. Biol. Chem.* **277**, 23084–23091.
- Wang, C., Luosujärvi, H., Heikkinen, J., Risteli, M., Uitto, L. & Myllylä, R. (2002) *Matrix Biol.* **21**, 559–566.
- Gossler, A. & Zachgo, J. (1994) in *Gene Targeting: A Practical Approach*, ed. Joyner, A. L. (IRL, Oxford), pp. 182–227.
- Kivirikko, K. I. & Myllylä, R. (1982) *Methods Enzymol.* **82**, 245–304.
- Scacheri, P. C., Crabtree, J. S., Novotny, E. A., Garrett-Beal, L., Chen, A., Edgemon, K. A., Marx, S. J., Spiegel, A. M., Chandrasekharappa, S. C. & Collins, F. S. (2001) *Genesis* **30**, 259–263.
- Myllyharju, J. & Kivirikko, K. I. (2004) *Trends Genet.* **20**, 33–43.
- Timpl, R., Wiedemann, H., Van Delden, V., Furthmayr, H. & Kühn, K. (1981) *Eur. J. Biochem.* **120**, 203–211.
- Yurchenco, P. D. & Furthmayr, H. (1984) *Biochemistry* **23**, 1839–1850.
- Langeveld, J. P. M., Noelken, M. E., Hård, K., Todd, P., Vliegenhart, J. F. G., Rouse, J. & Hudson, B. G. (1991) *J. Biol. Chem.* **266**, 2622–2631.
- Norman, K. & Moerman, D. G. (2000) *Dev. Biol.* **227**, 690–705.
- Yurchenco, P. D., Amenta, P. S. & Patton, B. L. (2004) *Matrix Biol.* **22**, 521–538.
- Miner, J. H., Li, C., Mudd, J. L., Go, G. & Sutherland, A. E. (2004) *Development (Cambridge, U.K.)* **131**, 2247–2256.
- Smyth, N., Vatanserver, H. S., Murray, P., Meyer, M., Frie, C., Paulsson, M. & Edgar, D. (1999) *J. Cell Biol.* **144**, 151–160.
- Costell, M., Gustafsson, E., Aszodi, A., Mörgelin, M., Bloch, W., Hunziker, E., Addicks, K., Timpl, R. & Fässler, R. (1999) *J. Cell Biol.* **147**, 1109–1122.
- Pöschl, E., Schlötzer-Schrehardt, U., Brachvogel, B., Saito, K., Ninomiya, Y. & Mayer, U. (2004) *Development (Cambridge, U.K.)* **131**, 1619–1628.
- Halfter, W., Dong, S., Schurer, B., Osanger, A., Schneider, W., Ruegg, M. & Cole, G. J. (2000) *Dev. Biol.* **22**, 111–128.
- Dziadek, M., Darling, P., Bakker, M., Overall, M., Zhang, R.-Z., Pan, T.-C., Tillet, E., Timpl, R. & Chu, M.-L. (1996) *Exp. Cell Res.* **226**, 302–315.
- Myllyharju, J., Nokelainen, M., Vuorela, A. & Kivirikko, K. I. (2000) *Biochem. Soc. Trans.* **28**, 353–357.
- Nokelainen, M., Tu, H., Vuorela, A., Notbohm, H., Kivirikko, K. I. & Myllyharju, J. (2001) *Yeast* **18**, 797–806.